

Ice-sheet mass balance and climate change

Edward Hanna¹, Francisco J. Navarro², Frank Pattyn³, Catia M. Domingues⁴, Xavier Fettweis⁵, Erik R. Ivins⁶, Robert J. Nicholls⁷, Catherine Ritz⁸, Ben Smith⁹, Slawek Tulaczyk¹⁰, Pippa L. Whitehouse¹¹ & H. Jay Zwally¹²

Since the 2007 Intergovernmental Panel on Climate Change Fourth Assessment Report, new observations of ice-sheet mass balance and improved computer simulations of ice-sheet response to continuing climate change have been published. Whereas Greenland is losing ice mass at an increasing pace, current Antarctic ice loss is likely to be less than some recently published estimates. It remains unclear whether East Antarctica has been gaining or losing ice mass over the past 20 years, and uncertainties in ice-mass change for West Antarctica and the Antarctic Peninsula remain large. We discuss the past six years of progress and examine the key problems that remain.

This Review aims to synthesize the main advances in monitoring and modelling of ice-sheet mass balance since the publication of the 2007 Intergovernmental Panel on Climate Change Fourth Assessment Report¹ (IPCC AR4). Mass balance is defined as the net result of mass gains (primarily snow accumulation) and mass losses (primarily meltwater runoff and solid ice dynamical discharge across the grounding line). Surface mass balance (SMB) is the net balance of mass gains and losses at the ice-sheet surface and does not include dynamical mass loss. Efforts to determine ice-sheet mass balance using the three satellite geodetic techniques of altimetry, interferometry and gravimetry (see next section) have recently been sharpened by carefully defining common spatial and temporal domains for inter-comparison². Here we review the latest mass-balance estimates for the Antarctic Ice Sheet (AIS) and the Greenland Ice Sheet (GIS). New glacial isostatic adjustment (GIA) models, tested and evaluated against Global Positioning System (GPS) data, have recently led to significant downwards revision in GIA, and hence downwards revisions of gravimetric and altimetric satellite estimates of Antarctic mass loss² (Box 1).

Since the publication of IPCC AR4¹, ice-sheet models are no longer constrained to use overly simplified physics, allowing them to simulate more accurately the important coupling between ice sheets, ice streams and ice shelves. This major advance has been accompanied by improved model representation of the complex interactions of the ice sheet with its bed, the atmosphere and the ocean. For completeness, we also discuss briefly the contributions to sea-level rise (SLR) from other sources, namely glaciers and ice caps, thermal expansion of the oceans and terrestrial water storage changes. Despite recent advances, improved observations and predictions of ice-sheet response to climate change are as urgently needed to feed into mitigation and adaptation models of ensuing SLR as they were at the time of ref. 1.

Recent changes in ice-sheet mass balance Comparison of mass-balance estimates

One of the most sought after but elusive goals in contemporary Earth science is to relate the mass-balance state of the great ice sheets to observed SLR. A measure of this state provides an unambiguous quantification of

the ice-sheet system response to climate change. Recent mass-change estimates have been derived from three categories of techniques.

Volumetric techniques. These determine changes in the volume of the ice sheet via measurements of the height of the ice-sheet surface. They are based on radar altimetry^{3,4} or laser altimetry⁵.

Space gravimetric techniques. These derive changes in ice-sheet mass via repeated and very accurate measurement of the Earth's gravity field by the Gravity Recovery and Climate Experiment (GRACE) satellite system⁶.

BOX 1

Recent developments in GIA models

Glacial isostatic adjustment (GIA) is the response of the solid Earth, including associated changes in planetary gravity and rotation, to past redistributions of ice and ocean mass^{92,93}. The clearest observable effect of GIA is regional vertical rebound of the Earth's surface. Models of GIA are necessary for correcting measurements of present-day ice-mass change⁹⁴ and for long-term modelling⁴². The assimilation of glacial geological constraints on former ice extent and geodetic constraints on rebound into GIA models is helping to reduce the uncertainty associated with GIA, and hence estimates of ice-mass change^{11,12,95}. However, several key challenges remain. First, changes in ice extent and thickness during the past millennium are poorly known, and typically not included in GIA models, despite the fact that they can dominate the present-day rebound signal, especially in regions of low mantle viscosity^{96,97}. Second, lateral variations in Earth structure, as detected beneath Antarctica⁹⁸, also influence the GIA signal, but are not yet included in most models. Last, the limitations of the data used to tune GIA models mean that probabilistic approaches are now being adopted to seek the most likely range of solutions⁹⁹.

¹Department of Geography, University of Sheffield, Sheffield S10 2TN, UK. ²Departamento de Matemática Aplicada a las Tecnologías de la Información, Universidad Politécnica de Madrid, 28040 Madrid, Spain. ³Laboratoire de Glaciologie, Université Libre de Bruxelles, B-1050 Brussels, Belgium. ⁴Antarctic Climate and Ecosystems Cooperative Research Centre, University of Tasmania, Spendale, Victoria 3195, Australia. ⁵Department of Geography, University of Liège, 4000 Liège, Belgium. ⁶Jet Propulsion Laboratory, California Institute of Technology, Pasadena, California 91109-8099, USA. ⁷Faculty of Engineering and the Environment, University of Southampton, Southampton SO17 1BJ, UK. ⁸Laboratoire de Glaciologie et Géophysique de l'Environnement, UJF - Grenoble 1/CNRS, 38402 Saint-Martin d'Hères, France. ⁹Polar Science Center, Applied Physics Laboratory, University of Washington, Seattle, Washington 98105, USA. ¹⁰Department of Earth and Planetary Sciences, University of California, Santa Cruz, California 95064, USA. ¹¹Department of Geography, Durham University, Durham DH1 3LE, UK. ¹²NASA Goddard Space Flight Center, Cryospheric Sciences Laboratory, Greenbelt, Maryland 20771, USA.

Mass budget technique. This compares estimates of the net ice accumulation on the ice sheets with estimates of discharge across the grounding line⁷ (Box 2).

Each estimate relies on observational data that are unique to its own strategy, and each strategy, therefore, has a unique set of sensitivities to the errors and biases in its data. For example, mass budget^{7,8} studies use modelled snowfall fields from atmospheric reanalysis data^{9,10} to estimate the mass input into glacier basins, whereas radar and laser altimetry studies use the same fields to estimate the effective density of measured volume changes. Thus mass budget estimates have a first-order sensitivity to errors in the modelled mean accumulation rate, while radar and laser altimetry estimates have only limited sensitivity to errors in fluctuations in the accumulation rate.

Similarly, GRACE and radar and laser altimetry studies require the effects of GIA-related vertical bedrock motion (Box 1) to be removed accurately. Such vertical motion could be misinterpreted as ice-mass change by the GRACE satellites or as ice-thickness change by radar and laser altimeters, and a GIA correction must therefore be applied. This correction is a small percentage (~5%) of the total elevation change typically measured by altimeters; however, the GIA correction applied to GRACE data can be of the same order of magnitude as the signal due to contemporary ice-mass change (because of the density contrast between ice and the solid Earth). As a result, ambiguities in the GIA correction dominate GRACE sources of error in Antarctica (this is not as much of a problem for Greenland where the GIA correction is a much smaller fraction of the total mass change)⁶. Accurate quantification of the GIA signal is therefore crucial; small differences between models can alter the sign of the ice-mass change deduced from GRACE for individual drainage basins¹¹.

Published estimates of rates of Greenland and Antarctic ice-sheet mass change obtained using the above methods show a large spread of values for the past two decades (Fig. 1). Some of this spread is due to technical differences and some is due to different measurement epochs. However, in the past year, estimates have begun to give a more coherent picture for both Antarctica and Greenland. For Greenland, the trend of increasing mass loss (due to both SMB decrease and ice-to-ocean discharge increase) is clear, while some of the large mass loss estimates for Antarctica have been discarded. We describe some of the improvements in techniques and analysis below.

Reduced uncertainties

Recent assessments of mass-balance history^{12,13}, coupled with more robust GPS observations of the motion of exposed bedrock¹⁴, strongly suggest that Antarctic GIA-related bedrock motion peaks at about 5–6 mm yr⁻¹. The resulting GIA models for Antarctica^{13,15} deliver less than half the mass corrections implied by previous models. At the same time, processing of GRACE data has become more consistent between groups as the time series lengthens. Estimates using the latest models show moderate, if increasing, decadal mass losses for Antarctica^{13,16,17}.

In the IMBIE (Ice-sheet Mass Balance Inter-comparison Exercise) project, researchers recently compiled average sets of mass-balance estimates for common time periods for both the Antarctic and Greenland ice sheets, using the latest data, with multiple groups deriving estimates with each technique². An important technical change helped reduce the difference among techniques: unlike previously published mass budget estimates that extrapolated mass changes from surveyed to unsurveyed basins, the IMBIE mass budget estimates use radar altimetry data to demonstrate that unsurveyed areas have near-zero rates of mass change, giving, on average, less mass loss. Other extrapolation techniques can give a more positive Antarctic balance for the same data¹⁸. Similarly, including the most recent GIA estimates for Antarctica brought GRACE estimates closer to the radar and laser altimetry estimates. The IMBIE estimates are simple averages of all measurements, and the discordance that remains among methods (between radar and laser altimetry, for example) is not fully understood.

Figure 1 shows that the disparity of recent mass-balance results among different techniques—primarily from IMBIE—is considerably

BOX 2

Grounding lines and buttressing

Marine ice sheets, such as the West AIS, rest on bedrock that lies below sea level. These grounded ice sheets are fringed by floating ice shelves. The grounding line is the contact of the ice sheet with the ocean where the ice mass starts to float by buoyancy. Ice from the grounded ice sheet is discharged across the grounding line into ice shelves, from where icebergs break off, through a process called calving (Fig. 3).

The migration of the grounding line is a result of the local balance between the masses of ice and displaced ocean water. The grounding line advances if previously floating ice becomes thick enough to ground, or retreats if previously grounded ice becomes thin enough to float. Theory has demonstrated that in order to simulate grounding-line migration, it is necessary to include (horizontal) stress gradients across the grounding zone²² and in order to resolve this numerically, a high spatial resolution is needed, either by using a moving grid (following the grounding line directly) or by subsampling the grid around the grounding line to hundreds of metres (ref. 39). This high resolution is necessary to resolve horizontal stress gradients across a narrow boundary layer.

Ice discharge generally increases with increasing ice thickness at the grounding line. For a bed sloping down towards the interior this may lead to unstable grounding-line retreat, as increased flux (for example, due to reduced buttressing) leads to thinning and eventually flotation, which moves the grounding line into deeper water where the ice is thicker. Thicker ice results in increased ice flux, which further thins (and eventually floats) the ice, which results in further retreat into deeper water (and thicker ice), and so on (Fig. 3). This unstable retreat is referred to as the marine ice-sheet instability²². However, the grounding line is partially stabilized by the presence of ice shelves, which are either confined laterally through embayments or otherwise stabilized by locally grounded features which they enclose (for example, pinning points). Both geometries transmit a back-force, or 'buttressing', towards the grounded ice sheet, which may help to stabilize the grounding line against unstable retreat down inland-sloping bedrock¹⁰⁰.

Thinning of ice shelves reduces drag at the margins and over pinning points, leading to increased ice flow across the grounding line, causing grounding-line retreat until a new stable point (for example, upward sloping bedrock) is reached. The mechanisms described above rely heavily on a precise knowledge of the geometry of the ice-ocean contact, which explains why neighbouring outlet glaciers, in contact with the ocean, and subject to the same atmospheric and oceanic forcing, may exhibit contrasting behaviours³⁰.

reduced from that seen before. There tend to be systematic differences between the results from different techniques, with the mass budget method giving the most negative estimate for both ice sheets, laser altimetry the most positive, and GRACE in between. IMBIE radar altimetry estimates cover only the sub-peninsular part of Antarctica, and give rates of mass change consistent with those from GRACE. The techniques agree in sign, and roughly in magnitude, for Greenland, and there is considerable basin-scale spatial fidelity revealed in the inter-comparisons. Greenland had small contributions to SLR in the 1990s ($-51 \pm 65 \text{ Gt yr}^{-1}$) but was recently (2005–10) losing mass at $-263 \pm 30 \text{ Gt yr}^{-1}$ (ref. 2). (We note that $362.5 \text{ Gt yr}^{-1} = 1 \text{ mm yr}^{-1}$ sea-level equivalent.) The situation for Antarctica is less clear, with one estimate showing a significant positive mass balance¹⁹. An unweighted average of the estimates indicates that Antarctica, which was in a state of weakly negative balance in the 1990s, is now losing mass at a rate between -45 and -120 Gt yr^{-1} , with large dynamic losses in West Antarctica partially offset by SMB gains in East Antarctica.

For Greenland, an independent group of researchers compared laser altimetry, mass budget and GRACE estimates over the 2003–09 ICESat

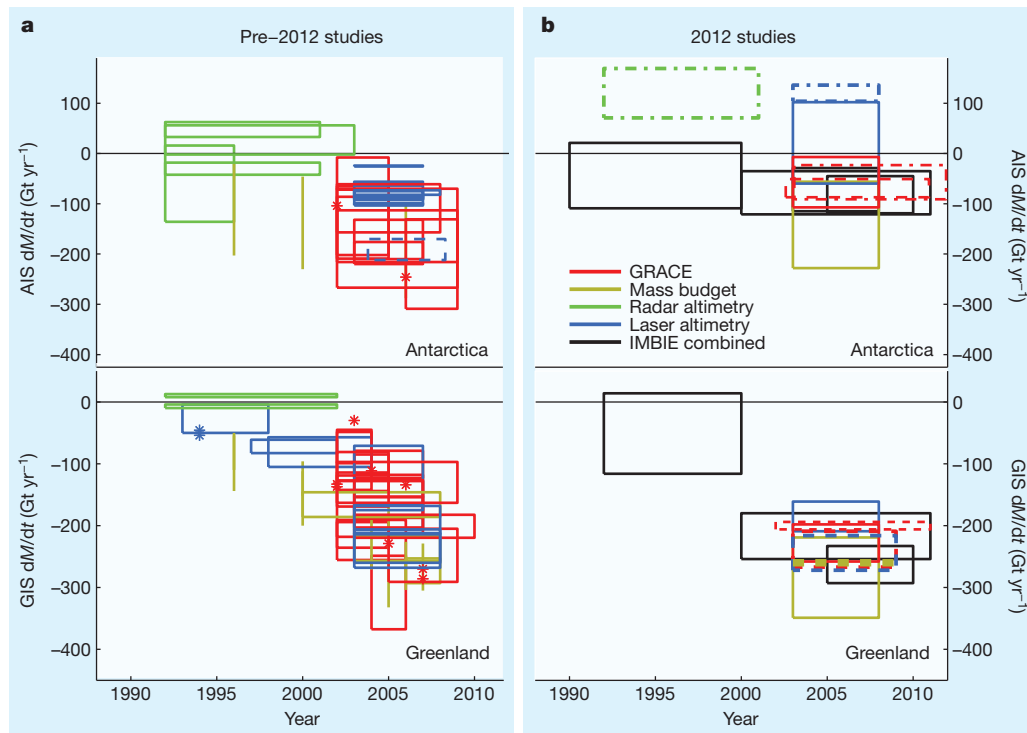


Figure 1 | Summary of estimates of rates of ice mass change for Antarctica and Greenland. In the studies published before 2012 (ref. 2, a) and in 2012 (b), each estimate of a temporally averaged rate of mass change is represented by a box whose width indicates the time period studied, and whose height indicates the error estimate. Single-epoch (snapshot) estimates of mass balance are represented by vertical error bars when error estimates are available, and are

otherwise represented by asterisks. Line colour indicates mass assessment technique (see key); line type indicates data source. 2012 studies in b comprise IMBIE combined estimates² (solid lines), and estimates by Sasgen and others^{16,20} and King and others¹¹ (dashed lines), Zwally and others¹⁹ (dot-dashed lines), Harig and Simons⁸⁹ and Ewert and others⁹⁰ (dotted lines).

(Ice, Cloud, and land Elevation Satellite) period: the mass budget estimate gave the maximum loss rates at $-260 \pm 53 \text{ Gt yr}^{-1}$ and GRACE the minimum, at $-238 \pm 29 \text{ Gt yr}^{-1}$ (ref. 20). On a basin-by-basin basis, agreement between the mass budget method and other techniques provides validation for the practice of partitioning mass-balance change between discharge and SMB components, demonstrating that in the northern part of Greenland, the dominant cause of mass change was atmospheric in origin, while in the southern part it was ice dynamics.

The new, reconciled IMBIE GRACE estimates of whole Antarctic mass balance are now largely in agreement with one another, with spreads of $30\text{--}50 \text{ Gt yr}^{-1}$ between the largest and smallest 2003–08 rates. Previously published GRACE values show spreads around twice as large for similar time periods. In the Antarctic Peninsula and West Antarctica, the IMBIE estimates from laser altimetry and GRACE are in good agreement, in contrast to East Antarctica². For East Antarctica, a mass gain of $+101 \text{ Gt yr}^{-1}$ for 2003–08 has been proposed recently on the basis of laser altimetry¹⁹, which is larger than the IMBIE GRACE estimate of $+35 \text{ Gt yr}^{-1}$ and near the upper end of the laser altimetry estimates².

Recent advances in ice-sheet modelling

Key improvements and future challenges

Significant improvements in ice-sheet modelling have been made since the publication of IPCC AR4¹, motivated by the need to understand continuing changes and by the challenge to make more realistic projections for the next few centuries. The primary improvements concern mechanical approximations made to the ice flow equations. The very first generation of ice-sheet models was based on the shallow ice approximation²¹. Such models assume that all resistance to flow is provided by shear-stress gradients in the vertical, which is valid for creeping ice-sheet flow, but not when other ice-dynamical features such as ice streams and ice sheet/ice shelf coupling come into play in ice-sheet

evolution. More recent ice-sheet models now include horizontal stress gradients, and can be classified into four categories of increasing complexity and computational cost. (1) Ice shelf/stream models are based on the shallow-shelf approximation²². They include horizontal stress gradients, but neglect the vertical shear stresses (which is valid for rapid ice flow at low basal traction). (2) Hybrid models use some combination of solutions from the shallow-ice approximation (to account for the vertical shearing component of flow within grounded ice) and the shallow-shelf approximation (to account for the horizontal stress coupling taking place in ice shelves or regions of rapid sliding)^{21,23,24}. (3) More elaborate higher-order models treat the vertical dimension more rigorously, with the only approximation being the hydrostatic assumption (pressure at any point in the ice is due only to the weight of the ice above it and not due to ice flow)^{25,26}. (4) Finally, a few models solve the equations of motion without neglecting any terms. These are called 'Full Stokes models', and have recently demonstrated their ability to perform century-timescale simulations applied to a whole ice sheet^{27,28}.

Spatial resolution of models is the second aspect that has been improved. Hardly any model is now run with a spatial grid size greater than 20 km, but this resolution is still not high enough to resolve ice streams, which are often only a few kilometres wide. Moreover, grounding-line migration and calving require subkilometre resolution. Unstructured grids (for finite element models^{27,28}) or adaptive mesh refinement²⁹ are two strategies that have proven efficient at treating this difficulty with acceptable computational cost.

A third improvement has been enabled through satellite and ground-based observations, such as the quantification of surface velocities and velocity change from satellite interferometry³⁰, surface elevation change through satellite and airborne campaigns (IceBridge), and high-resolution bedrock and ice thickness measurements³¹. Ice-sheet model behaviour is highly dependent on initial and boundary conditions and faces the difficulty that drag at the ice–bed interface is poorly known. Inverse methods

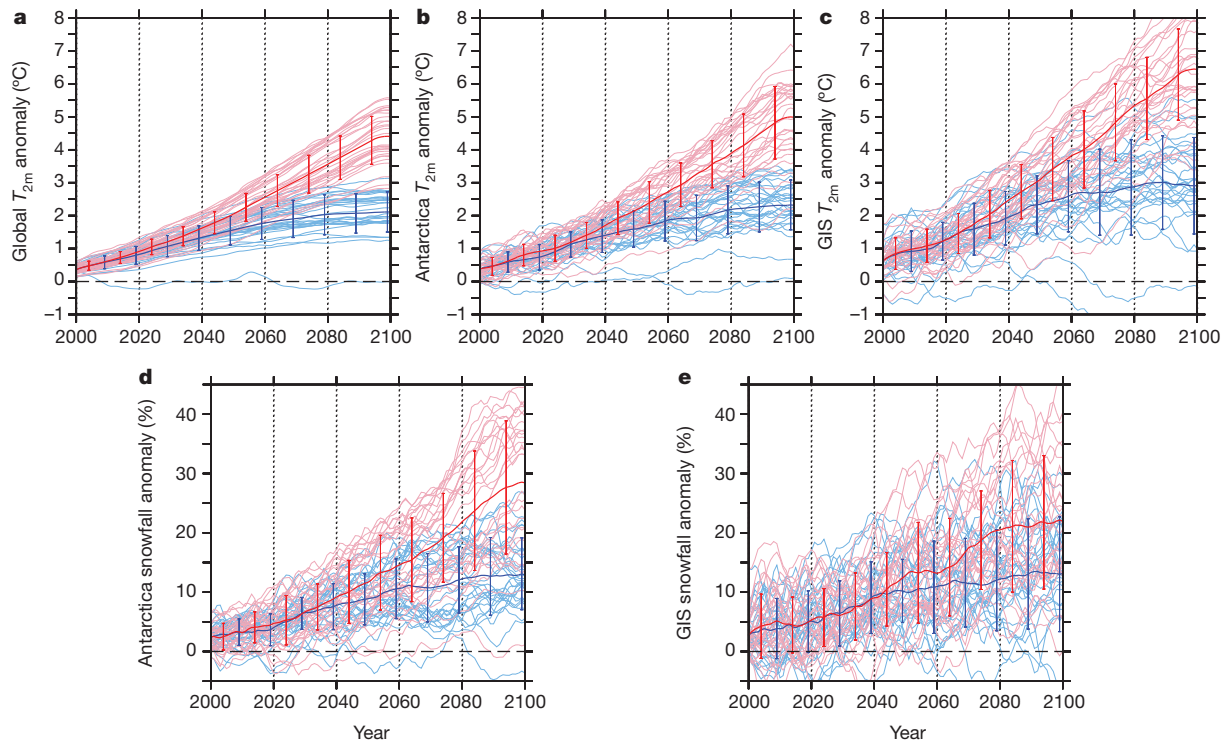


Figure 2 | Comparison of projected global, Antarctic and Greenland surface air temperature and snowfall anomalies to 2100. **a**, Anomaly of global mean 2 m air temperature (T_{2m}) simulated by 30 GCMs from the CMIP5 data base. Values are with respect to 1970–99 for the RCP 4.5 (blue) and RCP 8.5 (red) scenarios. We refer to ref. 91 for more details about the Representative Concentration Pathways (RCP) scenarios. The evolving ensemble means are plotted as thick lines, with vertical bars representing ± 1 s.d. for each decade.

have now been successfully implemented in ice-sheet models to infer the basal drag map that provides a good agreement between observed and simulated surface velocities. This procedure is becoming standard in the spin-up that is required for establishing an optimum initial state^{27–29,32}. All the above refinements enable models to reproduce present-day observed ice-sheet flow speeds, which is a major improvement since AR4¹ was published.

Grounding lines, sliding and calving

Warming-induced ice-shelf loss has caused major glaciers and ice streams of Antarctica to speed up^{33,34}. The mechanisms behind this speed-up are complex. Oceanic and/or atmospheric warming leads to ice-shelf thinning or disintegration^{35,36}, which in turn may lead to loss of buttressing³⁷, grounding-line retreat and hence glacier speed-up³³ (Box 2). Observations from the Antarctic Peninsula and the Amundsen Sea Embayment in West Antarctica (for example, Pine Island and Thwaites glaciers, which are currently the main contributors of the AIS to SLR³⁸) support these mechanisms.

Major theoretical advances²² in understanding the motion and stability of the grounding line show that in the absence of buttressing (see Box 2), grounding lines retreat unstably on an upward-sloping bed (in the direction of ice flow). Analytical solutions are now available to test and verify marine ice-sheet models, so that the numerical error associated with predicting grounding-line motion can be reduced significantly to the level of parameter uncertainties³⁹: models that attempt to account for grounding-line dynamics should incorporate horizontal stress transmission across the grounding line, so that the grounded ice sheet realistically feels the influence of floating ice (Box 2). Furthermore, the grounding line needs to be resolved at a sufficiently high spatial resolution³⁹. Such developments have been made recently and applied to Pine Island glacier, where a small increase in sub-ice-shelf melting has been shown to result in either unstable grounding-line retreat²⁹,

A 10-year running mean was used to smooth the curves. **b**, Same as **a** but for Antarctica. The land/sea mask from each GCM is used to delimit Antarctica. **c**, Same as **a** but for T_{2m} over GIS. The T_{2m} anomaly is taken over the area covering Greenland (60–85° N and 20–70° W) and where surface elevation is higher than 1,000 m above sea level. **d**, Same as **b** but for precipitation. Anomalies are given in per cent with respect to the mean precipitation for 1970–99. **e**, Same as **c** but for precipitation.

or grounding-line stabilization approximately 25 km inland within 100 years (ref. 37).

GIA also influences ice-sheet behaviour^{40,41}. Effects such as Earth's deformation in response to ocean loading, and perturbations to the shape of the sea surface in response to the redistribution of both internal and surface masses, including changes to the mass of the ice sheet itself, play a key role in governing the behaviour of a marine-grounded ice sheet, such as West Antarctica⁴². GIA alters the water depth via spatially varying perturbations to both the ocean floor and the sea surface and this has a first-order effect on grounding-line positions²². Ignoring such processes can fundamentally alter model predictions relating to the stability of a marine-grounded ice sheet⁴¹.

Ice flow across the grounding line is equally controlled by inland basal hydrological conditions and processes that govern basal sliding and sediment deformation. A wide range of observations over the GIS suggests that surface melt water reaches the bed by fracture and drainage through moulins, and this is likely to affect basal lubrication⁴³. Recent work has shown that it is not simply mean surface melt but an increase in water input variability that drives faster ice flow⁴⁴. This has been confirmed by observations⁴⁵. However, more recent work supports the original contention that increased melt water leads to increases in basal sliding, but that the effect is much smaller than originally thought because of buffering by subglacial drainage system evolution⁴⁶. Given the available evidence, the representation of basal sliding in large-scale ice-sheet models still depends largely on empirical parameterizations based on observations of seasonal variations in ice flow.

Recent developments in the understanding of calving follow either fundamental process approaches^{47,48}, leading to global calving laws relating thickness at the grounding line/calving front to calving rate, or are based on stochastic modelling and fracture theory⁴⁹. Two-dimensional generalizations of similar calving laws have been proposed in large-scale models⁵⁰. More specific approaches take into consideration environmental factors,

relating surface meltwater runoff and sub-shelf melting to the widening of crevasses and subsequent calving⁵¹. However, model applications based on this approach remain restricted to one-dimensional flowline models⁵², owing to the lack of data to resolve the geometry of outlet glacier embayments at sufficiently high spatial resolution. Although improvements have been made over recent years, this lack of data hampers a complete process-based evaluation of calving. In the near future, it is likely that models will continue to rely on empirically based parameterizations of calving.

Future ice-sheet changes

For significantly warmer climates, both the GIS and AIS are projected to lose mass⁵³. General circulation models (GCMs) generally project a small increase of snowfall over both ice sheets (Fig. 2d, e). However, the mass loss from increasing surface melt will be dominant over the GIS. For Antarctica, although the SMB is projected to increase, there remain major uncertainties concerning the response of the marine ice sheets and ice shelves to ocean forcing.

Surface melt already occurs over a large part of the GIS during summer and reached a new record in 2012⁵⁴. Therefore, rising temperatures will mainly affect mass loss through increased surface melt in summer, and several positive feedbacks may accelerate this surface mass loss:

- (1) Polar amplification of global warming resulting from, among other processes, the decrease of sea-ice extent over the Arctic Ocean and its associated positive albedo feedback. This process, already observed in recent years⁵⁵ and simulated by the Coupled Model Inter-comparison Project Phase 5 (CMIP5) GCMs (see Fig. 2c compared with Fig. 2a), doubles the estimated uncertainties in projected near-surface temperature anomalies for Greenland compared with those at the global scale⁵⁶.
- (2) Positive snow albedo feedback over the ice sheet itself associated with the expansion of the bare ice zone. This effect explains why the meltwater runoff increases quadratically with rising summer temperatures: the albedo of bare ice (0.3–0.5) is much less than that of melting snow (~0.7), and surface melt water becomes more likely to run off rather than percolating into deeper parts of the snowpack⁵⁷.
- (3) Positive elevation feedbacks associated with the thinning of the ice sheet resulting from the increasing surface melt and ice discharge. Significant thinning (up to 100 m) of the ice sheet is projected along the ice-sheet margin⁵⁸, which should cause an additional melt increase over this area (as ice moves to lower elevations, where it is warmer).

Dynamical changes of the GIS due to enhanced lubrication, calving and ocean warming still remain difficult to predict. Higher-order ice flow modelling of observed retreat of GIS glaciers over the past decade and subsequent upscaling (extrapolation of these model results to the whole GIS) leads to a minimum additional SLR of 6 ± 2 mm by 2100, with an upper bound of 45 mm when recurring forcing is applied⁵⁹, while similar upscaling of realistic atmospheric and oceanic forcing of four GIS glaciers with a calving model leads to a maximum dynamic contribution of 40–85 mm by 2100⁶⁰. This is still lower than previous estimates, but higher than when this retreat chronology is implemented in a three-dimensional higher-order model, leading to a dynamic contribution of 7–15 mm (ref. 61). The reason for such low numbers is that owing to the retreat of the ice-sheet margin, calving seems to decrease in relative importance^{53,61}. According to a model inter-comparison⁶², increased ice shelf melt rates of 2 m yr^{-1} lead to 27 mm SLR by 2100 (and 135 mm from a high melt rate of 20 m yr^{-1}). In response to SMB changes, ice-sheet model results are quite consistent and most studies conclude that the largest uncertainty comes from the spread among global climate models, which is amplified by some of the above-mentioned feedbacks over Greenland^{56,58}.

For Antarctica, the amplification of the global climate modelling uncertainties is smaller and the contribution of Antarctica to SLR is predicted to increase logarithmically with rising global temperatures (as positive feedbacks become increasingly apparent later) but with little change, and even perhaps a negative contribution, in the next 100–200 years (ref. 53). First, polar amplification resulting from reduced sea-ice coverage seems to be smaller than for the Arctic (see Fig. 2b).

However, a changing Antarctic Circumpolar Current could potentially allow warmer water to penetrate into the coastal shelf regions of Antarctica—as is observed⁶³. Second, little surface melt currently occurs and rising temperatures are not expected to enhance surface melt significantly in the next 100 years (ref. 53). Third, an increase in snowfall is expected to be more significant owing to atmospheric temperature rise, hence leading to an increase in SMB⁶⁴. Here, the elevation feedback resulting from SMB changes is negative because the ice sheet is initially projected to thicken⁵³, which is expected to affect its dynamics, especially on longer than centennial timescales.

The response of ice-sheet dynamics is twofold, due to increased accumulation and to higher ocean temperatures (in particular below the ice shelves). Two models^{53,65} produce ice-sheet thickening over East Antarctica and increased ice flux at the grounding line due to higher snowfall. However, both studies^{53,65} fail to account for processes at the ice-sheet/ice shelf/ocean interface, such as grounding-line retreat or loss of buttressing³⁹. So far, a continental-scale Antarctic ice-sheet model assessment taking into account those fundamental processes is lacking, although one assessment—based on a wide variety of model complexities—does report large inter-model variability in response to ocean forcing⁶². Process-based modelling of parts of the West AIS, such as Pine Island glacier, results in a SLR contribution of 27 mm by 2100 for a modest grounding-line retreat of 25 km (ref. 37), whereas significant (100 km) grounding-line retreat is modelled elsewhere²⁹. An alternative method based on probabilistic extrapolation of sustained glacier retreat from such numerical model output³⁷ leads to a SLR contribution of 130 mm by 2100⁶⁶.

Other contributions to SLR

The global average rate of SLR over the past few decades is about $2\text{--}3 \text{ mm yr}^{-1}$ (ref. 67). Estimates of the global contribution from glaciers and ice caps (GICs) to SLR in the IPCC AR4¹, $0.50 \pm 0.18 \text{ mm yr}^{-1}$ (1961–2003) and $0.77 \pm 0.22 \text{ mm yr}^{-1}$ (1993–2003), were based on extrapolation of sparse mass-balance measurements made by the glaciological method¹ (Box 3). These values were later considered underestimates⁶⁸, owing to the poor representation in the glacier inventories of the GICs peripheral to Greenland and Antarctica (peripheral GICs, PGICs): thus the 1961–2003 value was raised, based on a combined modelling and observations approach⁶⁸, to $0.79 \pm 0.34 \text{ mm yr}^{-1}$ (no value was provided for 1993–2003). A later extrapolation-based global estimate⁶⁹, with the novelty of allowing explicitly for glacier shrinkage, resulted in a lower estimate of 0.63 mm yr^{-1} for 1961–2006 (no uncertainty was given). The extrapolation-based global estimates have been improved by the addition of geodetic mass balances (Box 3) to the inventories of mass balance calculated using the glaciological method, which has resulted in consistently larger contributions to SLR, especially for the

BOX 3

Glaciological versus geodetic method

GIC mass-balance estimates by the glaciological method are based on extrapolation over the whole glacier surface of measurements of accumulation and ablation made *in situ* at single points. These measurements include readings of surface elevation changes at stakes, sampling of density and accumulation in pits and shallow cores, depth probing of the snow and firn, and shallow coring.

Estimates by the geodetic method are based on repeated mapping of glacier surface elevations to estimate the volume changes, from which the mass changes are calculated using information about the density of the material and its time variations. The elevation changes can be measured using different techniques, either from the glacier surface or, more commonly, from airborne or satellite-borne sensors.

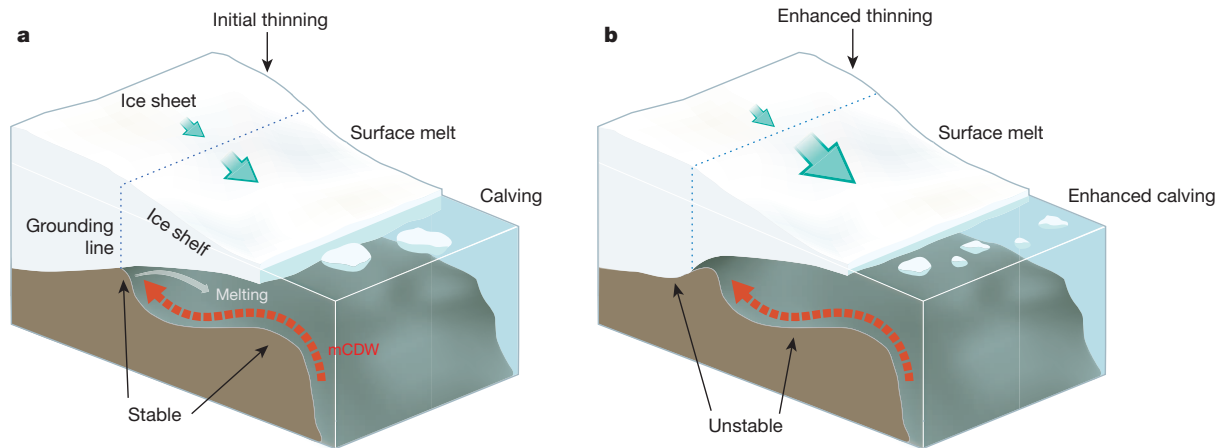


Figure 3 | Illustration of a marine ice sheet and its interaction with the ocean. **a**, Warm modified Circumpolar Deep Water (mCDW) leads to melting at the grounding line, leading to ice-sheet thinning, grounding-line retreat, and initial thinning. **b**, Marine ice-sheet instability occurs when, in the absence of buttressing, the grounding line retreats on an upward-sloping (in the direction

of the flow) bedrock (unstable): ice flux increases with thickness at the grounding line, leading to an increased outflux to the ocean and enhanced thinning that may be compensated by further grounding-line retreat, until a new downward-sloping bed (pinning point) is reached (stable). Thinning of ice sheet and shelf can also be caused by surface melt and increased calving.

most recent periods (for example, 0.99 ± 0.04 and 1.46 ± 0.34 mm yr^{-1} for 1993–2008 and 2000–05, respectively^{67,70}, compared with 0.97 and 0.95 mm yr^{-1} for 1993–2006 and 2002–06 respectively⁶⁹). Satellite gravimetry, a method traditionally restricted to the large ice sheets, has recently been used to estimate the global contribution of GICs to SLR⁷¹. GRACE data alone do not have the resolution to separate the Greenland and Antarctic ice sheets from their PGICs, but using an upscaling approach similar to that of ref. 68 has allowed one group to estimate a global contribution from GICs to SLR of 0.63 ± 0.23 mm yr^{-1} during 2003–10⁷¹, which is 30% and 47% lower than the two previous estimates that most closely match this period (2002–06⁶⁹ and 2005–10⁷², respectively). GRACE results for GICs, however, are sensitive to the models used for calculating GIA, post-Little Ice Age isostatic rebound, and surface- and ground-water mass transfer corrections.

The large uncertainties associated with the conventional extrapolation-based methods mostly arise from the uneven representation of the glacier-covered regions in the mass-balance measurements and the incomplete knowledge of the PGICs, both in terms of poorly known mass balances and inaccurate estimates of their area. The latter has greatly improved with the recent release of the Randolph Glacier Inventory⁷³. A consensus estimate combining GRACE, laser altimetry and the extrapolation-based method, using a common inventory of glaciers and a common spatial and temporal reference⁷⁴, has very recently enabled reconciliation of the disparate global estimates of wastage from GICs so far available from the different techniques. The consensus value is 0.71 ± 0.08 mm yr^{-1} during 2003–09, which is far lower than the extrapolation-based approach⁷² and somewhat higher than the GRACE-based estimate⁷¹.

Ocean thermal expansion (OTE) is a major component of the SLR observed during the late twentieth century⁶⁷, and is projected to continue through the twenty-first century and beyond⁷⁵. The IPCC AR4 found that OTE contributed $\sim 25\%$ of the observed SLR for 1961–2003 and $\sim 50\%$ for 1993–2003¹. Time-varying biases in the ocean temperature data, however, were recently detected⁷⁶ and reduced. It is now understood that the percentages of SLR explained by OTE during the above periods are almost identical⁷⁷, and so are higher for 1961–2003 and lower for 1993–2003 than estimated in the IPCC AR4¹. A recent sea level budget⁶⁷ indicates that OTE contributed $\sim 40\%$ of the observed SLR since 1970 and $\sim 30\%$ since 1993. Warming in the upper 700 m of the ocean explains about 70–80% of the OTE rates. Multi-decadal rates⁷⁷ for OTE in the upper 700 m are 0.71 ± 0.10 mm yr^{-1} for 1970–2011 and 0.85 ± 0.20 mm yr^{-1} for 1993–2011, based on linear regression and time-variable uncertainties. Multi-decadal rates for the deep/abysal

ocean are very uncertain⁶⁷, as these are the most poorly sampled regions of the ocean. Since 2005, about 3,000 autonomous Argo profiling floats have been monitoring the upper 2,000 m of the ocean. The Argo-based OTE rate⁷⁸ for 2005–11 is 0.60 ± 0.20 mm yr^{-1} , in close agreement with the change inferred from satellite altimetry and GRACE⁷⁹. Although consistent with the rates estimated for the multi-decadal periods, the OTE rate for 2005–11 is unlikely to represent long-term changes. Over such a short period, long-term changes can be easily obscured by more energetic ocean variability, such as fluctuations in the phase of the El Niño/Southern Oscillation⁸⁰.

Recent estimates for total terrestrial water storage changes during 1993–2008, which include dam retention, groundwater depletion and natural terrestrial storage changes, give values ranging from -0.08 ± 0.19 mm yr^{-1} (ref. 67) to 0.10 ± 0.20 mm yr^{-1} (ref. 81). A much larger (positive) contribution dominated by groundwater depletion has recently been suggested⁸², although this result is still controversial⁸³.

Table 1 summarizes the recent and current contributions to SLR calculated with the methods discussed in this Review and compares their sum with the observed SLR from tide gauges and satellite altimetry⁶⁷. OTE appears as the main current contributor to SLR, closely followed by the large ice sheets, whose contribution is increasing, and the GICs. The contribution from land-ice masses (ice sheets and GICs) could be

Table 1 | Estimated recent and current contributions to SLR

Source of contributions	SLR (mm yr^{-1})	
	1992/93 to 2008/11*	2000/03 to 2009/11*
GIS + AIS ²	0.59 ± 0.20	0.82 ± 0.16
GICs ^{72,74}	1.40 ± 0.16	0.71 ± 0.08
Ocean thermal expansion ^{77,87,88}	1.10 ± 0.43	1.11 ± 0.80
Terrestrial water storage (1993–2008) ^{67,81}	0.02 ± 0.26	
Sum of contributions	3.11 ± 0.56	2.66 ± 0.86
Observed (1993–2008) ⁶⁷	3.22 ± 0.41	

For 'Terrestrial water storage' and 'Observed', only the values for the longer time span are given; the terrestrial water storage number is used for the sum of contributions for both periods; 'Observed' means observed SLR from tide gauges and satellite altimetry. For GICs we have taken an update of the values given in ref. 72 for 1993–2011, while for 2003–09 we have used the value given in ref. 74. The value given for 'Ocean thermal expansion' combines a long-term abyssal value⁸⁷ with updates, for the periods shown in the table, from an average of refs 77 and 88 for the uppermost 700 m, and from ref. 88 for 0–2,000 m. The value given for terrestrial water storage is an average of those in the references shown. The uncertainties given are the published errors from the individual studies (usually standard deviations). When data from several sources are combined, the quoted error for the sum of contributions is the square root of the sum of the individual variances.

*The two periods given here need to accommodate data from a variety of sources, and so flexible start and finish dates are given. For example, '1992/93 to 2008/11' means that the data in the column below start in 1992 or 1993, and end somewhere between 2008 and 2011.

slightly overestimated, because only some of the methods in the consensus estimate for ice sheets² explicitly exclude the PGICs (and thus the contribution from PGICs may have been double-counted). Also, the apparent decrease in the contribution from the GICs between the two periods (Table 1) is mostly a result of the different methods used, rather than a result of a lower SMB observed during 2005–10⁷² (to illustrate this, we note that the GICs SLR contribution given in ref. 72 for 2000–10 is $1.38 \pm 0.21 \text{ mm yr}^{-1}$). Note that, for the most recent period, there is a gap between the sum of contributions and the SLR observed from tide gauges and satellite altimetry.

Conclusions and outlook

During the past 20 years, the AIS as a whole (East, West and Antarctic Peninsula) has been losing mass, and this is certainly true of the GIS². There are still disagreements between the numbers that come from the mass-balance retrieval techniques, particularly for East Antarctica, demonstrating a need to understand the errors of each method better. For radar altimetry, further assessment is needed of surface-density corrections and of short-term corrections to ENVISat radar altimetry data⁸⁴, as more moderate estimates of rates of mass change are possible using such corrections. For the mass budget method, NASA's IceBridge project will provide airborne-radar-based improvements to SMB estimates, and radar-sounding measurements of ice thickness at grounding lines will provide improved discharge estimates. Gravimetry and laser altimetry will have, respectively, GRACE and ICESat-2 follow-on missions (scheduled launches in 2017 and 2016, respectively) that will ideally provide a decadal record of whole ice-sheet mass balance. However, it is unlikely that these refinements will change the consensus picture emerging: whereas Antarctica as a whole is losing mass slowly (assessed to be contributing 0.2 mm yr^{-1} sea-level equivalent by IMBIE²), Greenland, the Antarctic Peninsula and parts of West Antarctica are together losing mass at a moderate ($\sim 1 \text{ mm yr}^{-1}$ sea-level equivalent) rate today ($\sim 70\%$ of this mass loss is from Greenland) and rates for each are becoming increasingly negative. For the past decade, the collective sea-level contribution from the ice sheets is similar to those from each of GICs and oceanic thermal expansion.

Although the West AIS is most probably going to continue to contribute to SLR (although the amount is poorly constrained), the sign of the contribution of the East AIS over the next century is uncertain. From the standpoint of projecting global sea level through this century and beyond, it is of fundamental importance to focus on improving ice-sheet models, including representation of key processes and nonlinear transitions. The concern of policymakers rightly focuses on the possibility of extreme outcomes, with their large impact potential and adaptation need⁸⁵. This is particularly true for the cryosphere, which responds nonlinearly to rising temperatures because of several potential positive feedbacks that may accelerate deglaciation. Improved knowledge of key ice-sheet thresholds would support climate policy decisions. Continued observations of ice-sheet processes and their implementation in ice-sheet models are crucial to ensure more accurate sea-level projections.

We have identified several important challenges that remain. First, there is a need for upscaling parameterizations to allow low-resolution models, which run fast but with coarse meshes, to represent crucial processes better. So far, parameterizations for grounding-line migration have been proposed^{122,23} and tested against more complete models³⁹. Although advances have been made on the theoretical level, process-based calving implemented in numerical flow models still has to rely on parameterizations that are not fully verified against physical models. Second, although progress has been achieved in the spin-up of ice-sheet models so that initial states are closer to observations through the use of inversion techniques, the nonlinearity of basal drag and its dependency on basal hydrology remains a concern. Time-dependent evolution of basal drag is not yet fully implemented in operational models, partly because subglacial hydrology models have not yet been fully implemented and partly because the data required to calibrate spatially dependent basal friction laws are lacking. The recent release of velocity maps for

various time periods⁸⁶ gives hope that this problem will soon be tackled. Third, a further vital step will be to couple improved ice-sheet models with atmosphere/ocean models and GIA models to account for all the feedbacks between the various physical systems at sufficiently high resolution. This will need to be supported by targeted observations with appropriate spatial and temporal coverage.

Received 3 January; accepted 26 April 2013.

1. Solomon, S., et al. *Contribution of Working Group I to the Fourth Assessment Report of the Intergovernmental Panel on Climate Change* (Cambridge Univ. Press, 2007).
2. Shepherd, A. et al. A reconciled estimate of ice sheet mass balance. *Science* **338**, 1183–1189 (2012).
Gives an overall view of remote sensing of ice-sheet mass balance and arrives at a nearly reconciled estimate of the contribution of the ice sheets to sea-level rise.
3. Davis, C. H. & Li, Y. H. McConnell, J. R., Frey, M. M. & Hanna, E. Snowfall-driven growth in East Antarctic ice sheet mitigates recent sea-level rise. *Science* **308**, 1898–1901 (2005).
4. Zwally, H. J. et al. Mass changes of the Greenland and Antarctic ice sheets and shelves and contributions to sea-level rise: 1992–2002. *J. Glaciol.* **51**, 509–527 (2005).
5. Zwally, H. J. et al. Greenland ice sheet mass balance: distribution of increased mass loss with climate warming. *J. Glaciol.* **57**, 88–102 (2011).
6. Velicogna, I. Increasing rates of ice mass loss from the Greenland and Antarctic ice sheets revealed by GRACE. *Geophys. Res. Lett.* **36**, L19503 (2009).
7. Rignot, E. & Kanagaratnam, P. Changes in the velocity structure of the Greenland ice sheet. *Science* **311**, 986–990 (2006).
8. Rignot, E., Velicogna, I., van den Broeke, M. R., Monaghan, A. & Lenaerts, J. Acceleration of the contribution of the Greenland and Antarctic ice sheets to sea level rise. *Geophys. Res. Lett.* **38**, L05503 (2011).
9. Ettema, J. et al. Higher surface mass balance of the Greenland ice sheet revealed by high-resolution climate modeling. *Geophys. Res. Lett.* **36**, L12501 (2009).
10. Lenaerts, J. T. M., van den Broeke, M. R., van de Berg, W. J., van Meijgaard, E. & Munneke, P. K. A new, high-resolution surface mass balance map of Antarctica (1979–2010) based on regional atmospheric climate modeling. *Geophys. Res. Lett.* **39**, L04501 (2012).
11. King, M. A. et al. Lower satellite-gravimetry estimates of Antarctic sea-level contribution. *Nature* **491**, 586–589 (2012).
12. Whitehouse, P. L., Bentley, M. J. & Le Brocq, A. M. A deglacial model for Antarctica: geological constraints and glaciological modelling as a basis for a new model of Antarctic glacial isostatic adjustment. *Quat. Sci. Rev.* **32**, 1–24 (2012).
13. Ivins, E. R. et al. Antarctic contribution to sea-level rise observed by GRACE with improved GIA correction. *J. Geophys. Res.* <http://dx.doi.org/10.1002/jgrb.50208> (in the press).
14. Thomas, I. D. et al. Widespread low rates of Antarctic glacial isostatic adjustment revealed by GPS observations. *Geophys. Res. Lett.* **38**, L22302 (2011).
15. Whitehouse, P. L., Bentley, M. J., Milne, G. A., King, M. A. & Thomas, I. D. A new glacial isostatic adjustment model for Antarctica: calibrated and tested using observations of relative sea-level change and present-day uplift rates. *Geophys. J. Int.* **190**, 1464–1482 (2012).
Demonstrates that new GIA models for Antarctica, which have been central to reconciling mass-balance estimates, greatly improve the fit between modelled and observed (GPS) uplift rates.
16. Sasgen, I. et al. Antarctic ice-mass balance 2002 to 2011: regional re-analysis of GRACE satellite gravimetry measurements with improved estimate of glacial-isostatic adjustment. *Cryosphere Discuss.* **6**, 3703–3732 (2012).
17. Horwath, M., Legresy, B., Remy, F., Blarel, F. & Lemoine, J. M. Consistent patterns of Antarctic ice sheet interannual variations from ENVISAT radar altimetry and GRACE satellite gravimetry. *Geophys. J. Int.* **189**, 863–876 (2012).
18. Zwally, H. J. & Giovinetto, M. B. Overview and assessment of Antarctic ice-sheet mass balance estimates: 1992–2009. *Surv. Geophys.* **32**, 351–376 (2011).
19. Zwally, H. J. et al. Mass balance of Antarctic ice sheet 1992 to 2008 from ERS and ICESat: gains exceed losses. *ISMAS 2012 Workshop* (2012); available at <http://www.climate-cryosphere.org/en/events/2012/ISMAS/AntarcticIceSheet.html>.
20. Sasgen, I. et al. Timing and origin of recent regional ice-mass loss in Greenland. *Earth Planet. Sci. Lett.* **333–334**, 293–303 (2012).
21. Ritz, C., Rommelaere, V. & Dumas, C. Modeling the evolution of Antarctic ice sheet over the last 420 000 years: implications for altitude changes in the Vostok region. *J. Geophys. Res.* **106**, 31943–31964 (2001).
22. Schoof, C. Ice sheet grounding line dynamics: steady states, stability, and hysteresis. *J. Geophys. Res.* **112**, F03S28 (2007).
23. Pollard, D. & Deconto, R. M. Modelling West Antarctic ice sheet growth and collapse through the past five million years. *Nature* **458**, 329–332 (2009).
24. Bueler, E. & Brown, J. Shallow shelf approximation as a “sliding law” in a thermomechanically coupled ice sheet model. *J. Geophys. Res.* **114**, F03008 (2009).
25. Pattyn, F. A new three-dimensional higher-order thermomechanical ice sheet model: basic sensitivity, ice stream development and ice flow across subglacial lakes. *J. Geophys. Res.* **108** (B8), 2382 (2003).
26. Blatter, H. Velocity and stress fields in grounded glaciers: a simple algorithm for including deviatoric stress gradients. *J. Glaciol.* **41**, 333–344 (1995).
27. Gillet-Chaulet, F. et al. Greenland Ice Sheet contribution to sea-level rise from a new-generation ice-sheet model. *Cryosphere* **6**, 1561–1576 (2012).

- Represents the first complete implementation of full Stokes in dynamical ice-sheet models.**
28. Larour, E., Seroussi, H., Morlighem, M. & Rignot, E. Continental scale, high order, high spatial resolution, ice sheet modeling using the Ice Sheet System Model (ISSM). *J. Geophys. Res.* **117**, F01022 (2012).
29. Cornford, S. L. *et al.* Adaptive mesh, finite volume modeling of marine ice sheets. *J. Comput. Phys.* **232**, 529–549 (2013).
- A complete and correct implementation of 3D grounding line dynamics applied to Pine Island glacier for a loss of ice shelf buttressing, uniquely showing large grounding-line retreat.**
30. Moon, T. & Joughin, I. Smith, B. & Howat, I. 21st-century evolution of Greenland outlet glacier velocities. *Science* **336**, 576–578 (2012).
31. Gogineni, P. CReSIS Data Products. <http://data.cresis.ku.edu/> (2012).
32. Arthern, R. J. & Gudmundsson, G. H. Initialization of ice-sheet forecasts viewed as an inverse Robin problem. *J. Glaciol.* **56**, 527–533 (2010).
33. Scambos, T. A., Bohlander, J. A., Shuman, C. A. & Skvarca, P. Glacier acceleration and thinning after ice shelf collapse in the Larsen B embayment, Antarctica. *Geophys. Res. Lett.* **31**, L18402 (2004).
34. Rignot, E. *et al.* Recent ice loss from the Fleming and other glaciers, Wordie Bay, West Antarctic Peninsula. *Geophys. Res. Lett.* **32**, L07502 (2005).
35. Jacobs, S. S., Jenkins, A., Giulivi, C. F. & Dutriex, P. Stronger ocean circulation and increased melting under Pine Island Glacier ice shelf. *Nature Geosci.* **4**, 519–523 (2011).
36. MacAyeal, D. R., Scambos, T. A., Hulbe, C. L. & Fahnestock, M. A. Catastrophic ice-shelf break-up by an ice-shelf-fragment-capsize mechanism. *J. Glaciol.* **49**, 22–36 (2003).
37. Joughin, I., Smith, B. E. & Holland, D. M. Sensitivity of 21st century sea level to ocean-induced thinning of Pine Island Glacier, Antarctica. *Geophys. Res. Lett.* **37**, L20502 (2010).
38. Rignot, E. *et al.* Recent Antarctic ice mass loss from radar interferometry and regional climate modelling. *Nature Geosci.* **1**, 106–110 (2008).
39. Pattyn, F. *et al.* Grounding-line migration in plan-view marine ice-sheet models: results of the ice2sea MISIP3d intercomparison. *J. Glaciol.* (in the press).
- A community inter-comparison exercise that shows the capabilities of current ice-sheet models for robustly simulating grounding-line migration, which is key for predicting marine ice-sheet behaviour.**
40. Greischar, L. L. & Bentley, C. R. Isostatic equilibrium grounding line between the West Antarctic inland ice-sheet and the Ross ice shelf. *Nature* **283**, 651–654 (1980).
41. Gomez, N., Mitrova, J. X., Huybers, P. & Clark, P. U. Sea level as a stabilizing factor for marine-ice-sheet grounding lines. *Nature Geosci.* **3**, 850–853 (2010).
42. Gomez, N., Pollard, D., Mitrova, J. X., Huybers, P. & Clark, P. U. Evolution of a coupled marine ice sheet-sea level model. *J. Geophys. Res.* **117**, F01013 (2012).
43. Das, S. B. *et al.* Fracture propagation to the base of the Greenland ice sheet during supraglacial lake drainage. *Science* **320**, 778–781 (2008).
44. Schoof, C. Ice sheet acceleration driven by melt supply variability. *Nature* **468**, 803–806 (2010).
- Shows the important role of the ice sheet–ice shelf transition zone in controlling marine ice-sheet dynamics (in particular, stability/instability).**
45. Sundal, A. *et al.* Melt-induced speed-up of Greenland ice sheet offset by efficient subglacial drainage. *Nature* **469**, 521–524 (2011).
46. Bartholomew, I. *et al.* Short-term variability in Greenland Ice Sheet motion forced by time-varying meltwater drainage: implications for the relationship between subglacial drainage system behavior and ice velocity. *J. Geophys. Res.* **117**, F03002 (2012).
47. Amundson, J. & Truffer, M. A unifying framework for iceberg-calving models. *J. Glaciol.* **56**, 822–830 (2010).
48. Hindmarsh, R. C. A. An observationally validated theory of viscous flow dynamics at the ice-shelf calving front. *J. Glaciol.* **58**, 375–387 (2012).
49. Bassis, J. N. The statistical physics of iceberg calving and the emergence of universal calving laws. *J. Glaciol.* **57**, 3–16 (2011).
50. Levermann, A. *et al.* Kinematic first-order calving law implies potential for abrupt ice-shelf retreat. *Cryosphere* **6**, 273–286 (2012).
51. Benn, D. I., Warren, C. R. & Mottram, R. H. Calving processes and the dynamics of calving glaciers. *Earth Sci. Rev.* **82**, 143–179 (2007).
52. Nick, F. M., Vieli, A., Howat, I. M. & Joughin, I. Large-scale changes in Greenland outlet glacier dynamics triggered at the terminus. *Nature Geosci.* **2**, 110–114 (2009).
53. Goelzer, H. *et al.* Millennial total sea-level commitments projected with the Earth system model of intermediate complexity LOVECLIM. *Environ. Res. Lett.* **7**, 045401 (2012).
54. Nghiem, S. V. *et al.* The extreme melt across the Greenland ice sheet in 2012. *Geophys. Res. Lett.* **39**, L20502 (2012).
- Key paper documenting this large-scale Greenland melt event that was unprecedented in the modern satellite record.**
55. Screen, J. A., Deser, C. & Simmonds, I. Local and remote controls on observed Arctic warming. *Geophys. Res. Lett.* **39**, L10709 (2011).
- Provides strong observational and model evidence of symptoms and causes of the recent amplified Arctic warming.**
56. Yoshimori, M. & Abe-Ouchi, A. Sources of spread in multimodel projections of the Greenland ice sheet surface mass balance. *J. Clim.* **25**, 1157–1175 (2012).
57. Harper, N., Humphrey, N. F., Pfeffer, W. T., Brown, J. & Fettweis, X. Greenland ice-sheet contribution to sea-level rise buffered by meltwater storage in firn. *Nature* **491**, 240–243 (2012).
58. Fettweis, X. *et al.* Estimating Greenland ice sheet surface mass balance contribution to future sea level rise using the regional atmospheric climate model MAR. *Cryosphere* **7**, 469–489 (2013).
59. Price, S. F., Payne, A. J., Howat, I. M. & Smith, B. E. Committed sea-level rise for the next century from Greenland ice sheet dynamics during the past decade. *Proc. Natl Acad. Sci. USA* **108**, 8978–8983 (2011).
60. Nick, F. M. *et al.* Future sea-level rise from Greenland's main outlet glaciers in a warming climate. *Nature* **497**, 235–238 (2013).
61. Goelzer, H. *et al.* Sensitivity of Greenland ice sheet projections to model formulations. *J. Glaciol.* (in the press).
62. Bindshadler, R. A. *et al.* Ice sheet model sensitivities to environmental forcing and their use in projecting future sea level (the SeaRISE project). *J. Glaciol.* **59**, 195–224 (2013).
63. Arneborg, L., Wåhlin, A. K., Björk, G., Liljebladh, B. & Orsi, A. H. Persistent inflow of warm water onto the central Amundsen shelf. *Nature Geosci.* **5**, 876–880 (2012).
64. Bengtsson, L., Koumoutsaris, S. & Hodges, K. Large-scale surface mass balance of ice sheets from a comprehensive atmospheric model. *Surv. Geophys.* **32**, 459–474 (2011).
65. Winkelmann, R., Levermann, A., Martin, M. A. & Frieler, K. Increased future ice discharge from Antarctica owing to higher snowfall. *Nature* **492**, 239–242 (2012).
66. Little, C., Oppenheimer, M. & Urban, N. M. Upper bounds on twenty-first-century Antarctic ice loss assessed using a probabilistic framework. *Nature Clim. Change* <http://dx.doi.org/10.1038/nclimate1845> (published online 17 March 2013).
67. Church, J. A. *et al.* Revisiting the Earth's sea-level and energy budgets from 1961 to 2008. *Geophys. Res. Lett.* **38**, L18601 (2011).
- A good and recent (though the numbers are already outdated in many cases) review of all contributions to SLR.**
68. Hock, R., de Woul, M., Radić, V. & Dyurgerov, M. Mountain glaciers and ice caps around Antarctica make a large sea-level rise contribution. *Geophys. Res. Lett.* **36**, L07501 (2009).
69. Dyurgerov, M. B. Reanalysis of glacier changes: from the IGY to the IPY, 1960–2008. *Data Glaciol. Studies* **108**, 5–116 (2010).
70. Cogley, J. G. Geodetic and direct mass-balance measurements: comparison and joint analysis. *Ann. Glaciol.* **50**, 96–100 (2009).
71. Jacob, T., Wahr, J., Pfeffer, W. T. & Swenson, S. Recent contributions of glaciers and ice caps to sea level rise. *Nature* **482**, 514–518 (2012).
72. Cogley, J. G. in *The Future of the World's Climate* 2nd edn (eds Henderson-Sellers, A. & McGuffie, K.) 197–222 (Elsevier, 2012).
73. Arendt, A. *et al.* *Randolph Glacier Inventory: A Dataset of Global Glacier Outlines Version 2.0* (GLIMS Technical Report, Global Land Ice Measurements from Space, Boulder, 2012); available at <http://www.glims.org/RGI/>.
74. Gardner, A. S. *et al.* A reconciled estimate of glacier contributions to sea level rise: 2003 to 2009. *Science* **340**, 852–857 (2013).
- Presents a consensus estimate of the contributions of glaciers and ice caps to sea-level rise that reconciles the disparate estimates previously available from the different techniques.**
75. Meehl, G. A. *et al.* Relative outcomes of climate change mitigation related to global temperature versus sea level rise. *Nature Clim. Change* **2**, 576–580 (2012).
76. Gouretski, V. & Koltermann, K. P. How much is the ocean really warming? *Geophys. Res. Lett.* **34**, L01610 (2007).
77. Domingues, C. M. *et al.* Improved estimates of upper-ocean warming and multi-decadal sea-level rise. *Nature* **453**, 1090–1093 (2008).
78. von Schuckmann, K. & Le Traon, P.-Y. How well can we derive global ocean indicators from Argo data? *Ocean Sci. Discuss* **8**, 999–1024 (2011).
79. Leuliette, E. W. & Willis, J. K. Balancing the sea level budget. *Oceanography (Wash. DC)* **24**, 122–129 (2011).
80. Roemmich, D. & Gilson, J. The global ocean imprint of ENSO. *Geophys. Res. Lett.* **38**, L13600 (2011).
81. Wada, Y. *et al.* Past and future contribution of global groundwater depletion to sea-level rise. *Geophys. Res. Lett.* **39**, L09402 (2012).
82. Pokhrel, Y. N. *et al.* Model estimates of sea-level change due to anthropogenic impacts on terrestrial water storage. *Nature Geosci.* **5**, 389–392 (2012).
83. Konikow, L. F. Overestimated water storage. *Nature Geosci.* **6**, 3–4 (2012).
84. Remy, F., Flament, T., Blarel, F. & Benveniste, J. Radar altimetry measurements over Antarctic ice sheet: a focus on antenna polarization and change in backscatter problems. *Adv. Space Res.* **50**, 998–1006 (2012).
85. Nicholls, R. J. *et al.* Sea-level rise and its possible impacts given a 'beyond 4°C world' in the twenty-first century. *Proc. R. Soc. Lond. A* **369**, 161–181 (2011).
86. Joughin, I., Smith, B., Howat, I., Scambos, T. & Moon, T. Greenland flow variability from ice-sheet-wide velocity mapping. *J. Glaciol.* **56**, 415–430 (2010).
87. Purkey, S. G. & Johnson, G. C. Warming of global abyssal and deep Southern Ocean waters between the 1990s and 2000s: contributions to global heat and sea level rise budgets. *J. Clim.* **23**, 6336–6351 (2010).
88. Levitus, S. *et al.* World ocean heat content and thermocline sea level change (0–2000 m), 1955–2010. *Geophys. Res. Lett.* **39**, L10603 (2012).
89. Harig, C. & Simons, F. J. Mapping Greenland's mass loss in space and time. *Proc. Natl Acad. Sci. USA* **109**, 19934–19937 (2012).
90. Ewert, H., Groh, A. & Dietrich, R. Volume and mass changes of the Greenland ice sheet inferred from ICESat and GRACE. *J. Geodyn.* **59–60**, 111–123 (2012).
91. Moss, R. H. *et al.* The next generation of scenarios for climate change research and assessment. *Nature* **463**, 747–756 (2010).
92. Farrell, W. E. & Clark, J. A. On postglacial sea level. *Geophys. J. R. Astron. Soc.* **46**, 647–667 (1976).
93. Kendall, R. A., Mitrova, J. X. & Milne, G. A. On post-glacial sea level — II. Numerical formulation and comparative results on spherically symmetric models. *Geophys. J. Int.* **161**, 679–706 (2005).
94. Wahr, J., Wingham, D. & Bentley, C. A method of combining ICESat and GRACE satellite data to constrain Antarctic mass balance. *J. Geophys. Res.* **105**, 16279–16294 (2000).

95. Simpson, M. J. R., Wake, L., Milne, G. A. & Huybrechts, P. The influence of decadal- to millennial-scale ice mass changes on present-day vertical land motion in Greenland: Implications for the interpretation of GPS observations. *J. Geophys. Res.* **116**, B02406 (2011).
96. Dietrich, R. *et al.* Rapid crustal uplift in Patagonia due to enhanced ice loss. *Earth Planet. Sci. Lett.* **289**, 22–29 (2010).
97. Sato, T. *et al.* Reevaluation of the viscoelastic and elastic responses to the past and present-day ice changes in Southeast Alaska. *Tectonophysics* **511**, 79–88 (2011).
98. Morelli, A. & Danesi, S. Seismological imaging of the Antarctic continental lithosphere: a review. *Global Planet. Change* **42**, 155–165 (2004).
99. Tarasov, L., Dyke, A. S., Neal, R. M. & Peltier, W. R. A data-calibrated distribution of deglacial chronologies for the North American ice complex from glaciological modeling. *Earth Planet. Sci. Lett.* **315–316**, 30–40 (2012).
100. Gudmundsson, G. H. *et al.* The stability of grounding lines on retrograde slopes. *Cryosphere* **6**, 1497–1505 (2012).

Acknowledgements The work presented here is based on the Ice-Sheet Mass Balance and Sea Level (ISMAS) workshop that was held in Portland, Oregon, USA, on 14 July 2012. This workshop was jointly organized by the Scientific Committee on Antarctic Research (SCAR), the International Arctic Science Committee (IASC) and the World Climate Research Programme (WCRP), and was co-sponsored by the International Council for Science (ICSU), SCAR, IASC, WCRP, the International Glaciological Society (IGS) and the International Association of Cryospheric Sciences (IACS), with support from Climate and Cryosphere (CliC) and the Association of Polar Early Career Scientists (APECS).

Author Contributions E.H. coordinated the study, E.H., F.J.N. and F.P. led the writing, and all authors contributed to the writing and discussion of ideas.

Author Information Reprints and permissions information is available at www.nature.com/reprints. The authors declare no competing financial interests. Readers are welcome to comment on the online version of the paper. Correspondence and requests for materials should be addressed to E.H. (ehanna@sheffield.ac.uk).